Aging Cell (2005) **4**, pp1–12 Doi: 10.1111/j.1474-9728.2004.00136.x

Activation of the PI3K/Akt signal transduction pathway and increased levels of insulin receptor in protein repair-deficient mice

Christine Farrar,[1] Carolyn R. Houser[2,3] and Steven Clarke[1,2]

[1]Department of Chemistry and Biochemistry and the Molecular Biology Institute, 637 Paul D. Boyer Hall, 611 Charles E. Young Drive East, Los Angeles, CA 90095–1570, USA [2]Brain Research Institute, UCLA, Los Angeles, CA 90095, USA [3]Department of Neurobiology, UCLA, Los Angeles, California 90095 and Research Services, VA Greater Los Angeles Healthcare System, West Los Angeles, Los Angeles, CA 90073, USA

Summary

Protein L-isoaspartate (D-aspartate) *O*-methyltransferase is an enzyme that catalyses the repair of isoaspartyl damage in proteins. Mice lacking this enzyme (*Pcmt1*–/– mice) have a progressive increase in brain size compared with wild-type mice (*Pcmt1*+/+ mice), a phenotype that can be associated with alterations in the PI3K/Akt signal transduction pathway. Here we show that components of this pathway, including Akt, GSK3β and PDK-1, are more highly phosphorylated in the brains of *Pcmt1*–/– mice, particularly in cells of the hippocampus, in comparison with *Pcmt1*+/+ mice. Examination of upstream elements of this pathway in the hippocampus revealed that *Pcmt1*–/– mice have increased activation of insulin-like growth factor-I (IGF-I) receptor and/or insulin receptor. Western blot analysis revealed an approximate 200% increase in insulin receptor protein levels and an approximate 50% increase in IGF-I receptor protein levels in the hippocampus of *Pcmt1*–/– mice. Higher levels of the insulin receptor protein were also found in other regions of the adult brain and in whole tissue extracts of brain, liver, heart and testes of both juvenile and adult *Pcmt1*–/– mice. There were no significant differences in plasma insulin levels for adult *Pcmt1*–/– mice during glucose tolerance tests. However, they did show higher peak levels of blood glucose, suggesting a mild impairment in glucose tolerance. We propose that *Pcmt1*–/– mice have altered regulation of the insulin pathway, possibly as a compensatory response to altered glucose uptake or metabolism or as an adaptive response to a general accumulation of isoaspartyl protein damage in the brain and other tissues.

Key words: Akt, enlarged brain, IGF-I receptor, insulin receptor, isoaspartate, PCMT1.

Introduction

Protein L-isoaspartate (D-aspartate) *O*-methyltransferase (PCMT1) is a protein repair enzyme that initiates the conversion of spontaneously isomerized aspartyl residues to their normal configuration (Johnson *et al*., 1987; McFadden & Clarke, 1987; Brennan *et al*., 1994; Kim *et al*., 1999; Ingrosso *et al*., 2000; Chavous *et al*., 2001; Doyle *et al*., 2003; Lanthier & Desrosiers, 2004). In mammals, this enzyme is expressed in all tissues, with highest levels of expression in the brain and testes (Kim *et al*., 1997; Yamamoto *et al*., 1998). Recently, mice with a disrupted gene encoding this enzyme (*Pcmt1*–/– mice) were generated in order to study its physiological relevance in the mammalian system (Kim *et al*., 1997; Yamamoto *et al*., 1998; Ikegaya *et al*., 2001; Lowenson *et al*., 2001). As *Pcmt1*–/– mice age, they accumulate higher levels of isoaspartyl-containing polypeptides in all tissues examined as compared with levels in *Pcmt1*+/+ mice (Kim *et al*., 1997; Yamamoto *et al*., 1998; Lowenson *et al*., 2001). The most apparent phenotype in the *Pcmt1*–/– mice is the occurrence of seizures and an early death, which occurs at an average of 6 weeks of age following a severe seizure episode (Kim *et al*., 1997, 1999; Yamamoto *et al*., 1998). The limited survival of the *Pcmt1*–/– mice seems to be caused by the seizures, as histological examinations have not revealed any apparent pathological abnormalities in the heart, lung or other tissues examined (Kim *et al*., 1997, 1999; Yamamoto *et al*., 1998; Ikegaya *et al*., 2001).

In addition to substrate accumulation and the occurrence of seizures, *Pcmt1*–/– mice have enlarged brains, which occurs without significant macroscopic abnormalities such as hydrocephalus or brain tumors (Yamamoto *et al*., 1998). The increase in brain size was surprising as their neurons were expected to be more susceptible to necrosis or apoptosis, particularly as overexpression of PCMT1 was reported to protect cell cultures of primary mouse cortical neurons and COS1 cells from Bax-induced apoptosis (Huebscher *et al*., 1999). Despite this and the potentially excitotoxic conditions often associated with seizures, there have been no reports of significant cell loss in these mice. However, a few distinctive microscopic alterations in their neurons and glia have been described. For example, cortical pyramidal neurons of layer V of the precentral cortex often appear swollen with an abnormally ballooned nucleus and

Correspondence
Dr Steven Clarke, 637 Paul D. Boyer Hall, 611 Charles E. Young Drive East, Los Angeles, CA 90095–1570; USA. Tel.: +1 310 825 8754; fax: +1 310 825 1968; e-mail: clarke@mbi.ucla.edu

Accepted for publication *29 September 2004*

clearly demarcated nucleolus (Yamamoto *et al*., 1998). In the granule cells of the dentate gyrus, *Pcmt1–/–* mice have enlarged vacuoles and cytoplasmic swelling, particularly at the axon hillock (Ikegaya *et al*., 2001). Also within the hippocampal formation, astrocytes show marked swelling from their cell bodies to the processes surrounding blood vessels (Ikegaya *et al*., 2001). Although these abnormalities could, in part, contribute to the enlargement of local brain regions in these mice, they fail to account for the brain's generalized enlargement.

To determine the possible cause of the enlarged brain in *Pcmt1–/–* mice, we examined the phosphatidylinositide 3,4,5-trisphosphate kinase (PI3K)/Akt signal transduction pathway (Fig. 1), which is one of the main signaling routes utilized by cells to control their growth and survival (Datta *et al*., 1999; Kozma & Thomas, 2002). This pathway has been shown to be involved in other mouse models in which regional or generalized brain enlargement is a prominent phenotype, including mice lacking TSC-1 (Uhlmann *et al*., 2002), PTEN (Groszer *et al*., 2001), caspase-9 (Kuida *et al*., 1998), or p27kip1 (Fero *et al*., 1996) and mice overexpressing insulin-like growth factor-I (IGF-I) (Carson *et al*., 1993) or β-catenin (Chenn & Walsh, 2002) (indicated by bold or dashed lined boxes in Fig. 1). In this study, we examined the activation and protein levels of Akt and both downstream and upstream components of this pathway in the brains of *Pcmt1*+/+ and *Pcmt1–/–* mice.

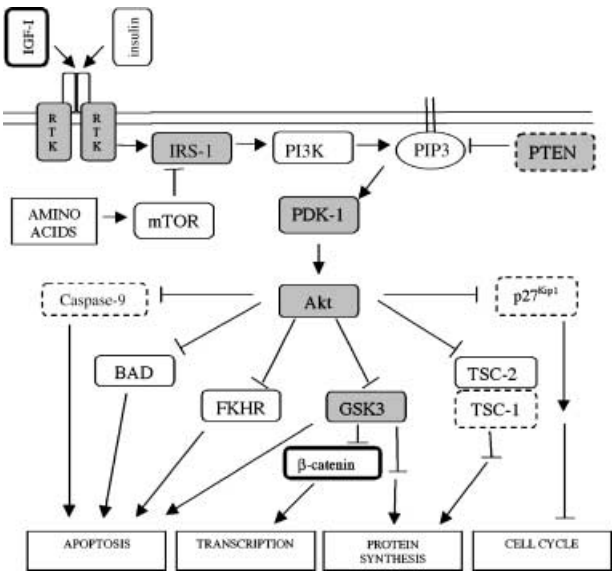

Fig. 1 PI3K/Akt signaling pathway. Arrows signify activation of function, and crossed lines signify deactivation of function. Dashed lined boxes represent proteins that have been found to result in regional or generalized enlargement in brains of mice when their expression is decreased *in vivo*. Bold lined boxes represent proteins that have been found to result in regional or generalized enlargement in brains of mice when their expression is increased *in vivo*. Shaded boxes signify proteins examined in this study. Abbreviations: RTK, receptor tyrosine kinase; IRS-1, insulin receptor substrate-1; PI3K, phosphatidylinositide 3-kinase; PIP3, phosphatidylinositide 3,4,5-trisphosphate; PDK-1, 3-phosphoinositide-dependent protein kinase-1; PTEN, phosphoinositide phosphatase (phosphatase and tensin homologue deleted from chromosome 10); mTOR, mammalian target of rapamycin; Akt, protein kinase B; GSK3, glycogen synthase kinase-3; TSC-1 & TSC-2, tuberous sclerosis complexes proteins 1 and 2; FKHR, Forkhead transcription factor; $p27^{Kip}$, cyclin D-CDK4/CDK6 kinase inhibitor of the Kip/Cip family.

Results

Increased weight of the hippocampus and cerebral cortex in *Pcmt1–/–* mice

As reported previously, *Pcmt1–/–* mice have an increase in brain size and weight compared with age-matched control mice without the occurrence of macroscopic abnormalities (Yamamoto *et al*., 1998). In this study, wet weight measurements of whole brain tissue showed an increase in brain weight for the *Pcmt1–/–* mice that was statistically significant and progressive from about 30–80 days of age (Fig. 2A). The brain weights of *Pcmt1–/–* mice were approximately 10% higher at 30 days of age and approximately 25% higher at 80 days of age as compared with brain weights of age-matched *Pcmt1*+/+ mice (Fig. 2B). Histological examinations of *Pcmt1–/–* mice in previous studies have indicated proportional enlargements in all brain areas, including the cerebral cortex, hippocampus, thalamus and cerebellum (Yamamoto *et al*., 1998). However, after examining the wet weight of different brain regions of 50-day-old mice, there was a 15–25% greater increase in the cerebral cortex and hippocampus than in other brain regions of *Pcmt1–/–* mice (Fig. 2C). Measurements of the per cent water content of brain tissue by dehydration indicated no significant difference between *Pcmt1–/–* and *Pcmt1*+/+ mice (Fig. 2D).

Increased activation of Akt in the hippocampus of *Pcmt1–/–* mice

To determine if the brain enlargement might involve increased activation of the PI3K/Akt pathway in *Pcmt1–/–* mice, we first examined the levels of activated Akt protein. As the hippocampus appears to have one of the greatest increases in weight and accumulation of microscopic abnormalities in *Pcmt1–/–* mice, Western blotting and immunohistochemical studies were focused on this region.

Akt is a serine/threonine kinase that is activated by phosphorylation at threonine-308 by 3-phosphoinositide-dependent protein kinase-1 (PDK-1) (Alessi *et al*., 1997; Stephens *et al*., 1998). Western blotting of hippocampal extracts using an antibody for Akt phosphorylated at threonine-308 showed an approximate 2.7-fold increase in immunoreactivity in *Pcmt1–/–* mice compared with *Pcmt1*+/+ mice, although the detection level was relatively low in all extracts (Fig. 3). Western blotting of hippocampal extracts using an antibody that detects total endogenous levels of Akt showed similar immunoreactivity in *Pcmt1–/–* and *Pcmt1*+/+ mice (Fig. 3). Western blotting using antibodies that detect actin also show similar levels in both *Pcmt1–/–* and *Pcmt1*+/+ mice (Fig. 3).

Although activation of Akt is dependent on phosphorylation at threonine-308, its activation can be enhanced 10-fold by phosphorylation at serine-473, which is believed to occur through

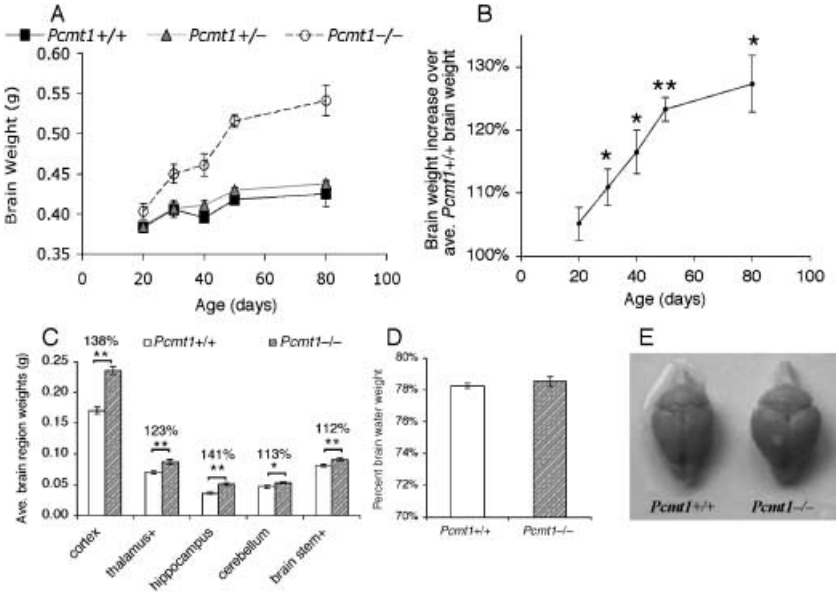

Fig. 2 Comparison of whole and regional brain weights of *Pcmt1*+/+ and *Pcmt1*–/– mice. (A) Brain weight values of *Pcmt1*+/+, *Pcmt1*+/– and *Pcmt1*–/– mice (n = 9, 8, 5, 23 and 2 for each group of mice at 20, 30, 40, 50, and 80 days, respectively). (B) Average brain weight values of *Pcmt1*–/– mice divided by average brain weight values of *Pcmt1*+/+ mice for the data shown in panel A. (C) Average brain region weight values for 50-day-old *Pcmt1*+/+ and *Pcmt1*–/– mice. The per cent average *Pcmt1*–/– brain region weight over that of average *Pcmt1*+/+ brain region weight is represented above each set of bars (n = 11 for all brain regions). (D) Average per cent brain tissue water weight for 50-day-old *Pcmt1*+/+ and *Pcmt1*–/– mice (n = 4 for each data set). (E) Picture of 50-day-old *Pcmt1*+/+ and *Pcmt1*–/– mouse brains. A–D, error bars represent ± SEM for all values, $*P < 0.05$ and $**P < 0.005$.

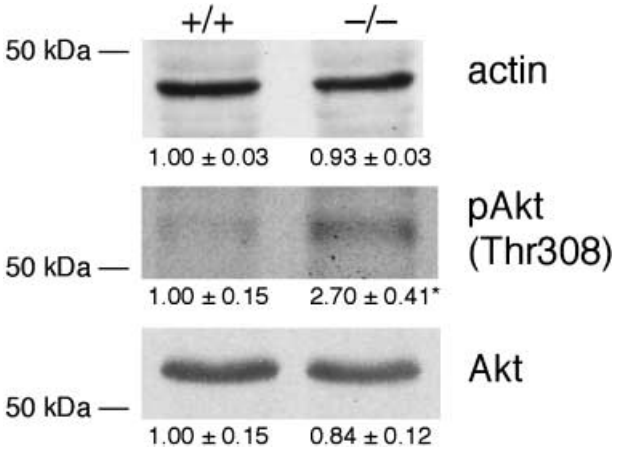

Fig. 3 Western blot analysis of phosphorylated Akt in the hippocampus of *Pcmt1*–/– and *Pcmt1*+/+ mice. The average density of bands obtained from *Pcmt1*+/+ tissue was normalized to a value of 1.00 and compared with the average density of bands obtained from *Pcmt1*–/– tissue. Values are shown below each blot ± SEM. Western blot analysis of hippocampal extracts using antisera against Akt phosphorylated at threonine-308 shows an increase in immunoreactivity for *Pcmt1*–/– compared with *Pcmt1*+/+ mice. Western blot analysis of hippocampal extracts using antisera against Akt and actin show similar immunoreactivity for *Pcmt1*–/– and *Pcmt1*+/+ mice (n = 4 for both *Pcmt1*+/+ and *Pcmt1*–/– mice, $*P < 0.05$).

both autophosphorylation and phosphorylation by distinct serine kinases (Scheid & Woodgett, 2003). In immunohistochemical studies using an antibody against Akt phosphorylated at serine-473, immunoreactivity was substantially increased in the dentate gyrus and CA3 region of the hippocampus in *Pcmt1*–/– mice (Fig. 4C,D). The increased labeling in the dentate gyrus was evident in the cell bodies of granule cells throughout the layer (Fig. 4E,F). The increased labeling in the CA3 region was seen in pyramidal cell bodies as well as in their proximal dendrites (Fig. 4G,H). An increase in immunoreactivity was also detected in the cerebral cortex, including neurons of the piriform cortex (data not shown). Control experiments with antibodies to actin displayed a similar pattern and intensity of labeling in *Pcmt1*–/– and *Pcmt1*+/+ mice (Fig. 4A,B). Additional controls where no primary antibody was used showed no detectable labeling in sections from either type of mice (data not shown).

Increased levels and phosphorylation of the downstream Akt target, GSK3β, in the hippocampus of *Pcmt1*–/– mice

One of the major downstream targets of the Akt kinase is glycogen synthase kinase-3 beta (GSK3β), which is involved in the regulation of a number of substrates affecting cellular metabolism, protein synthesis and cell survival (Cross *et al*., 1995; Srivastava & Pandey, 1998; Datta *et al*., 1999). In *Pcmt1*+/+ mice, immunolabeling of GSK3β in the hippocampal formation was generally low except for slightly higher labeling in the mossy fiber path that extends from the dentate gyrus into stratum lucidum of CA3 (Fig. 5A). In *Pcmt1*–/– mice, immunolabeling of GSK3β was substantially increased in the granule cell layer of the dentate gyrus and in the mossy fiber path (Fig. 5B). There was also a moderate increase in labeling in dendritic regions of the hippocampus that included stratum radiatum and stratum oriens.

Immunolabeling for GSK3β phosphorylated at serine-9 in *Pcmt1*+/+ mice was generally low throughout the hippocampal formation (Fig. 5C). Labeling in the mossy fiber path and dendritic regions of the hippocampus of *Pcmt1*+/+ mice was less distinct for pGSK3β than for GSK3β (Fig. 5A,C). In *Pcmt1*–/– mice, immunolabeling for phosphorylated GSK3β was highly increased in the dentate granule cell layer, mossy fiber path and dendritic regions of the hippocampus (Fig. 5D) compared with labeling in *Pcmt1*+/+ mice (Fig. 5C). Increased labeling was also detected in many regions of the cerebral cortex (data not shown).

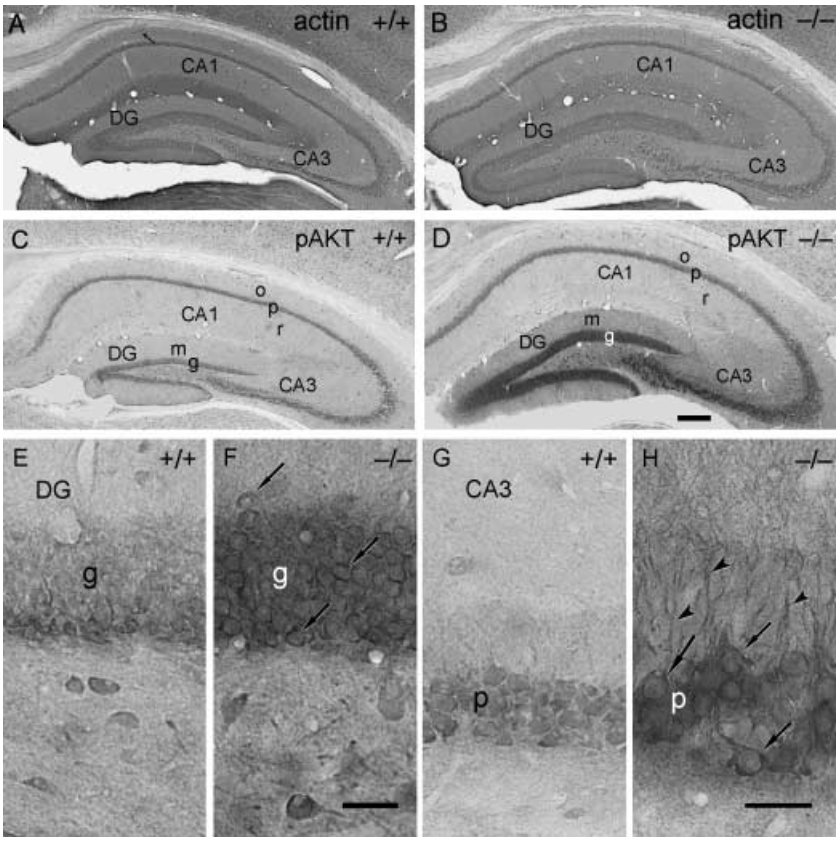

Fig. 4 Immunolabeling of actin and phosphorylated Akt in the hippocampus of *Pcmt1*+/+ and *Pcmt1*–/– mice by immunohistochemistry. (A–H) Coronal sections through the hippocampus of *Pcmt1*+/+ and *Pcmt1*–/– mice immunolabelled with antisera against actin (A,B) or Akt phosphorylated at serine-473 (C,H). (A,B) In control experiments, a similar pattern and intensity of actin labeling is observed in *Pcmt1*+/+ (A) and *Pcmt1*–/– (B) mice. (C) In *Pcmt1*+/+ mice, immunoreactivity is detected in the granule cells (g) of the dentate gyrus (DG) and pyramidal cells (p) of CA1–CA3. Labeling is low in dendritic regions that include the molecular layer (m), stratum radiatum (r) and the stratum oriens (o). (D) In *Pcmt1*–/– mice, there is an increase in immunoreactivity in the granule cells and molecular layer of the dentate gyrus and in the pyramidal cells of CA3. At higher magnification of the dentate gyrus (E and F), increased labeling is evident in the cell bodies throughout the granule cell layer (g) in *Pcmt1*–/– (F; examples at arrows) compared with *Pcmt1*+/+ mice (E). Higher magnification of CA3 pyramidal cells (G and H) shows increased labeling of cell bodies (arrows) and dendrites (arrowheads) in *Pcmt1*–/– (H) compared with *Pcmt1*+/+ mice (G). Scale bars: 200 μm (A–D), 25 μm (E–H).

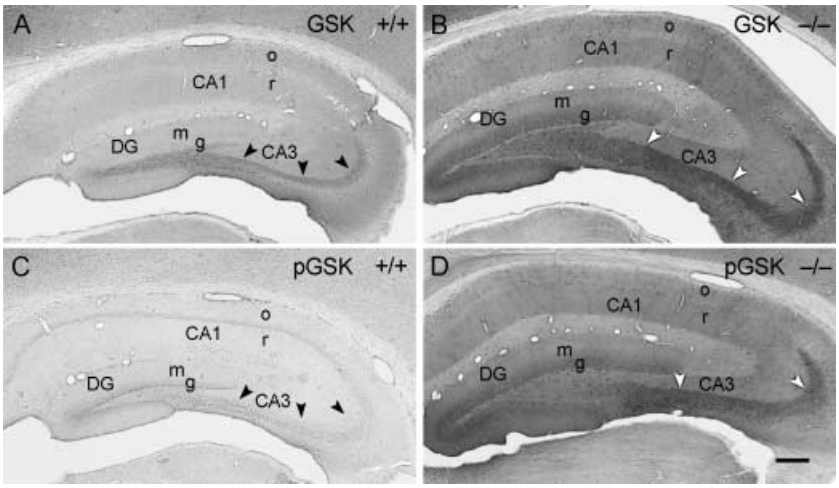

Fig. 5 Immunohistochemical labeling of the downstream signaling protein GSK3β in the hippocampus of *Pcmt1*+/+ and *Pcmt1*–/– mice. (A–D) Coronal sections through the hippocampus of *Pcmt1*+/+ and *Pcmt1*–/– mice immunolabelled with a polyclonal antibody against GSK3β (A and B) or GSK3β phosphorylated at serine-9 (C and D). (A) In *Pcmt1*+/+ mice, labeling of GSK3β is detected in the mossy fiber path (arrowheads). Only light labeling is present in dendritic regions that include the molecular layer (m), stratum radiatum (r) and stratum oriens (o). (B) In *Pcmt1*–/– mice, immunolabeling for GSK3β is increased in the mossy fiber path (arrowheads), granule cell layer (g) of the dentate gyrus (DG), stratum radiatum and stratum oriens, compared with *Pcmt1*+/+ mice (A). (C) In *Pcmt1*+/+ mice, immunolabeling of pGSK3β is very low in all subfields of the hippocampus, including the mossy fiber path (arrowheads). Labeling for pGSK3β (C) is lower than that for GSK3β (A) in *Pcmt1*+/+ mice. (D) In *Pcmt1*–/– mice, immunolabeling of pGSK3β is greatly increased in the mossy fiber path (arrowheads) and throughout the hippocampus compared with that in *Pcmt1*+/+ mice (C). The increased labeling for pGSK3β (D) is present in the same regions as those labelled for GSK3β (see B) in *Pcmt1*–/– mice. Scale bar: 200 μm (A–D).

Other phosphorylated downstream targets of Akt, such as pBAD and pFKHR, were examined by immunohistochemistry, and all demonstrated increased immunoreactivity in the hippocampus of *Pcmt1*–/– mice (data not shown). However, labeling for phosphorylated GSK3β demonstrated the most dramatic difference between the *Pcmt1*–/– and *Pcmt1*+/+ mice. It is possible that this is due to greater Akt phosphorylation of GSK3β than that of other downstream components, although phosphorylation by

additional kinase pathways (Srivastava & Pandey, 1998) and/or the increased levels of GSK3β protein may be contributing factors.

Altered levels of phosphorylated PDK-1 and PTEN in the hippocampus of *Pcmt1–/–* mice

Autophosphorylation in the kinase domain of PDK-1 at serine-241 is essential for its ability to phosphorylate Akt at threonine-308 (Casamayor *et al.*, 1999). Because this site is buried inside the protein, it is resistant to dephosphorylation by protein phosphatases (Steinberg *et al.*, 1993; Cheng *et al.*, 1998). This is especially important for analysis by Western blotting, as many of the proteins in brain homogenates may be susceptible to phosphatase activity during tissue processing. Western blots using an antibody for PDK-1 phosphorylated at serine-241 indicated an approximate 2.1-fold increase in phosphorylated PDK-1 in the hippocampus and an approximate 3.6-fold increase in the cortex of *Pcmt1–/–* mice compared with *Pcmt1*+/+ mice (Fig. 6).

PTEN resides at the plasma membrane where it dephosphorylates phosphatidylinositol 3,4-bisphosphate and phosphatidylinositide 3,4,5-trisphosphate, thus directly counteracting the effects of PI3K (Maehama & Dixon, 1998). The consequence of phosphorylation of PTEN at serine-380 is somewhat controversial. However, the prevailing view is that phosphorylation at this site gives PTEN stability but less activity, whereas dephosphorylation activates PTEN enhancing its ability to block Akt activity, but also targets it for degradation (Torres & Pulido, 2001; Vazquez *et al.*, 2001; Miller *et al.*, 2002). Western blots using an antibody for PTEN phosphorylated at serine-380 indicated a slight but significant decrease in phosphorylated PTEN in the hippocampus of *Pcmt1–/–* mice, whereas the levels in the cortex were relatively unchanged compared with *Pcmt1*+/+ mice (Fig. 6).

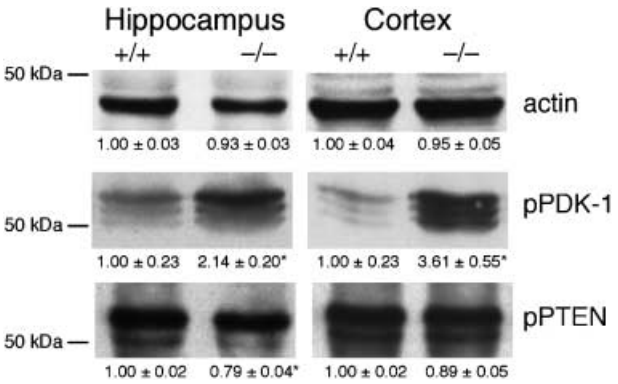

Fig. 6 Western blot analysis of the phosphorylated signaling proteins upstream of PI3K/Akt, pPDK-1 and pPTEN, in the hippocampus and cerebral cortex of *Pcmt1*+/+ and *Pcmt1–/–* mice. The average density of bands obtained from *Pcmt1*+/+ tissue was normalized to a value of 1.00 and compared with the average density of bands obtained from *Pcmt1–/–* tissue (n = 4 for hippocampal extracts of both *Pcmt1*+/+ and *Pcmt1–/–* mice for both antibodies, n = 3 for cortical extracts of both *Pcmt1*+/+ and *Pcmt1–/–* mice for pPDK-1, and n = 4 for pPTEN for cortical extracts of both *Pcmt1*+/+ and *Pcmt1–/–* mice). Values are shown below each blot ± SEM, *P = 0.05; Western blots using antibodies against actin were performed to ensure equal loading.

This result was important in demonstrating that increased phosphorylation seen in other elements of the PI3K/Akt pathway in the hippocampus of *Pcmt1–/–* mice was not simply a consequence of indiscriminate or general increases in phosphorylation.

Increased phosphorylation of IRS-1 and IGF-I receptor and/or insulin receptor in the hippocampus of *Pcmt1–/–* Mice

Based on our evidence that the PI3K/Akt signal transduction pathway is more highly activated in the hippocampus of *Pcmt1–/–* mice, we investigated the state of one of the upstream components, insulin receptor substrate-1 (IRS-1), which is a potent activator of the p85 subunit of PI3K (White, 1998). IRS-1 has at least ten tyrosine sites that can potentially be phosphorylated by receptor tyrosine kinases in response to various growth factors including IGF-I, insulin and, in some cells, IL-4 (White & Yenush, 1998). IRS-1 is phosphorylated at tyrosine-941 by IGF-I and insulin receptors and is one of the main binding sites for p85 (Xu *et al.*, 1995). Using an antibody for IRS-1 phosphorylated at tyrosine-941, *Pcmt1*+/+ mice showed relatively low labeling throughout the hippocampal formation except for moderate labeling along the inner border of the granule cell layer (Fig. 7A). In *Pcmt1–/–* mice, immunolabeling of pIRS-1 was slightly increased in this subgranular region and was substantially increased in the mossy fiber path compared with *Pcmt1*+/+ mice (Fig. 7B).

Type I insulin-like growth factor receptor (IGF-IR) and insulin receptor (IR) are transmembrane tyrosine kinases that share significant similarity in both structure and function. Upon binding of their individual ligands, autophosphorylation of the receptors' beta subunits occurs. The triple tyrosine clusters (Tyr1131, Tyr1135 and Tyr1136 for IGF-IR and Tyr1146, Tyr1150 and Tyr1151 for IR) within the kinase domain are the earliest major sites of autophosphorylation for both receptors (Hernandez-Sanchez *et al.*, 1995) and are necessary for their activation (White *et al.*, 1985, 1988; Baserga, 1999; Lopaczynski *et al.*, 2000). Using an antibody that detects both IGF-IR phosphorylated at Tyr1131 and IR phosphorylated at Tyr1146, we found increased immunoreactivity in virtually the same regions where increased labeling was detected for pIRS-I (Tyr941) when comparing *Pcmt1–/–* and *Pcmt1*+/+ mice (Fig. 7C,D). One of the most prominent increases in labeling occurred in the mossy fiber path, and at higher magnification, punctate structures, considered to be mossy fiber terminals, were darkly labelled in *Pcmt1–/–* mice (Fig. 7F) but undetectable in *Pcmt1*+/+ mice (Fig. 7E). Increased immunoreactivity for pIGF-IR/pIR was also detected in regions of the cerebral cortex in *Pcmt1–/–* mice (data not shown).

Increased insulin and IGF-I receptor protein levels in the hippocampus of *Pcmt1–/–* mice

The higher level of phosphorylation of the IGF-I/insulin receptor beta subunits seen in the hippocampus of *Pcmt1–/–* mice by immunohistochemistry may reflect increased protein levels and/

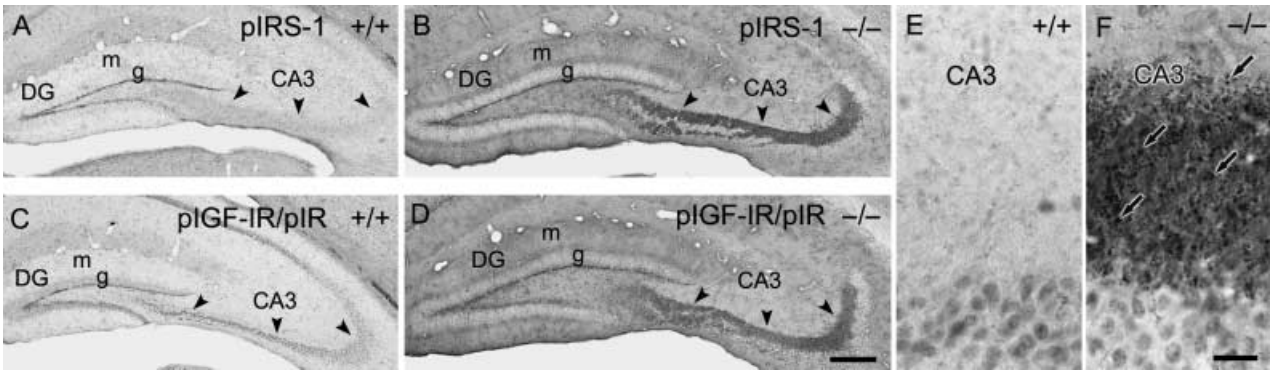

Fig. 7 Immunohistochemical labeling of the phosphorylated signaling proteins upstream of PI3K/Akt, IRS-I and IGF-IR/IR, in the hippocampus of *Pcmt1*+/+ and *Pcmt1*–/– mice. (A–F) Coronal sections through the hippocampus of *Pcmt1*+/+ and *Pcmt1*–/– mice immunolabelled with a polyclonal antibody against IRS-1 phosphorylated at tyrosine-941 (A and B) and IGF-IR phosphorylated at tyrosine-1131 and/or IR phosphorylated at tyrosine-1146 (C–F). (A) In *Pcmt1*+/+ mice, immunolabeling for pIRS-1 is detected along the inner border of the granule cell layer (g). labeling is low in the mossy fiber path (arrowheads) and in the molecular layer (m) of the dentate gyrus (DG). (B) In comparison with *Pcmt1*+/+ mice, *Pcmt1*–/– mice have substantially increased labeling for pIRS-1 in the mossy fiber path and molecular layer (m). (C) In *Pcmt1*+/+ mice immunolabeling for pIGF-IR/pIR is detected along the inner border of the granule cell layer (g) and in the pyramidal cells of CA1. Lighter labeling is detected in the granule cells of the dentate gyrus and the pyramidal cells of CA3. (D) immunolabeling for pIGF-IR/pIR in *Pcmt1*–/– mice is substantially increased in comparison with that in *Pcmt1*+/+ mice (C). The increased labeling shows a very similar pattern to that seen for pIRS-I in *Pcmt1*–/– mice, particularly in the mossy fiber path and along the inner border of the granule cell layer (compare panels B and D). (E,F) Higher magnification of the mossy fiber path in the CA3 region of *Pcmt1*+/+ and *Pcmt1*–/– mice immunolabelled for pIGF-IR/pIR. Punctate structures (arrows) that resemble axon terminals are strongly labelled in *Pcmt1*–/– mice (F) compared with *Pcmt1*+/+ mice (E). Scale bars: 200 μm (A–D), 25 μm (E,F).

or the relative activation of the receptors. To determine the comparative protein levels of the receptors in hippocampal and cortical extracts from the 50-day-old *Pcmt1*–/– and *Pcmt1*+/+ mice, Western blotting experiments were conducted using antibodies against the beta subunit of each receptor. Results from these experiments indicated increased levels of both IGF-IRβ and IRβ in hippocampal extracts of *Pcmt1*–/– mice compared with *Pcmt1*+/+ mice. However, whereas IGF-IRβ in the hippocampus of *Pcmt1*–/– mice showed only a 1.5-fold increase in protein levels over those in *Pcmt1*+/+ mice, IRβ showed a three-fold increase (Fig. 8). In the cortex, the *Pcmt1*–/– mice also had a three-fold increase in IRβ protein levels, but had no significant increase in IGF-IRβ protein levels compared with *Pcmt1*+/+ mice (Fig. 8).

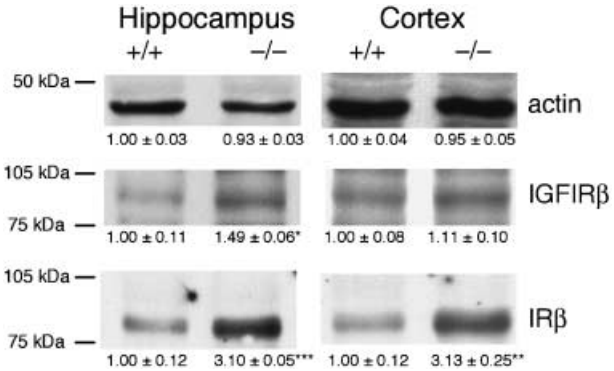

Fig. 8 Western blot analysis of IGF-I and insulin receptor levels in the hippocampus and cerebral cortex of *Pcmt1*+/+ and *Pcmt1*–/– mice. For all experiments, the average density of bands obtained from *Pcmt1*+/+ tissue was normalized to a value of 1.00 and compared with the average density of bands obtained from *Pcmt1*–/– tissue. Values are shown below each blot ± SEM. Using an antibody against the beta subunit of the IGF-I receptors (IGF-IRβ), hippocampal homogenates from *Pcmt1*–/– mice show an approximate 50% increase in labeling compared with *Pcmt1*+/+ mice. Cerebral cortex homogenates show no significant difference in labeling for IGF-IRβ. Both hippocampal and cerebral cortex homogenates show an approximate three-fold increase in labeling for IRβ in *Pcmt1*–/– compared with *Pcmt1*+/+ mice ($n = 4$ for both *Pcmt1*+/+ and *Pcmt1*–/– mice and for each antibody, $^*P < 0.05$, $^{**}P < 0.005$, and $^{***}P < 0.0005$; Western blots using antibodies against actin were performed to ensure equal loading).

Brain region and multi-tissue increases in insulin receptor protein levels in *Pcmt1*–/– mice

In order to examine the extent of the increased protein levels of IRβ in other brain areas of *Pcmt1*–/– mice, we conducted Western blotting experiments using extracts from the thalamus, cerebellum and brainstem of 50-day-old *Pcmt1*–/– and *Pcmt1*+/+ mice. The results from these experiments showed an approximate four-fold increase in receptor levels in thalamus and cerebellum extracts and an approximate 15-fold increase in brainstem extracts in *Pcmt1*–/– mice compared with *Pcmt1*+/+ mice (Fig. 9A). The greater degree of increase in these extracts compared with hippocampal and cortical extracts may be due to the low expression of IRβ protein found in hindbrain regions compared with rostral regions in the brains of normal animals (Baskin *et al*., 1987; Havrankova *et al*., 1978; Unger *et al*., 1989, 1991).

To determine the age at which IRβ protein levels started to increase in the brains of *Pcmt1*–/– mice, we conducted Western blotting experiments on whole brain extracts from 0-, 20- and 50-day-old *Pcmt1*–/– and *Pcmt1*+/+ mice. Our results indicated that by 20 days of age, IRβ protein levels in *Pcmt1*–/– mice were already approximately two-fold higher than those of age-matched *Pcmt1*+/+ mice (Fig. 9B). By 50 days of age, the level of IRβ protein in the *Pcmt1*–/– mouse brain showed an approximate three-fold increase over that of age-matched *Pcmt1*+/+

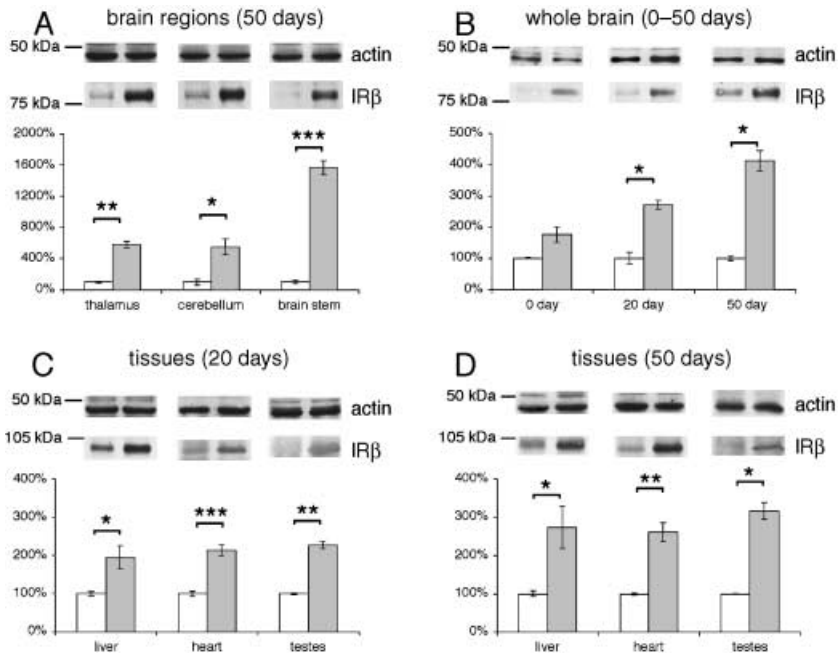

Fig. 9 Western blot analysis of insulin receptor levels in various tissues of *Pcmt1*+/+ and *Pcmt1*–/– mice. (A–D) Western blot analysis of tissue homogenates using an antibody against the beta subunit of insulin receptors (IRβ). (A) Homogenates of thalamus, cerebellum and brain stem from 50-day-old *Pcmt1*+/+ and *Pcmt1*–/– mice show a significant increase in labeling in each brain region examined for *Pcmt1*–/– compared with *Pcmt1*+/+ mice ($n = 4$ for both *Pcmt1*+/+ and *Pcmt1*–/– mice). (B) Whole brain homogenates from *Pcmt1*+/+ and *Pcmt1*–/– mice at 0, 20 and 50 days of age show a significant increase in protein levels for *Pcmt1*–/– mice at least as early as 20 days of age ($n = 2$ for both *Pcmt1*+/+ and *Pcmt1*–/– mice in each age group). (C) Homogenates of liver, heart and testes from 20-day-old *Pcmt1*+/+ and *Pcmt1*–/– mice show a significant increase in labeling in each tissue examined for *Pcmt1*–/– compared with *Pcmt1*+/+ mice ($n = 4$ for liver and heart from both *Pcmt1*+/+ and *Pcmt1*–/– mice; $n = 2$ for testes from both *Pcmt1*+/+ and *Pcmt1*–/– mice). (D) Homogenates of liver, heart and testes from 50-day-old *Pcmt1*+/+ and *Pcmt1*–/– mice show a significant increase in labeling in each tissue examined for *Pcmt1*–/– compared with *Pcmt1*+/+ mice. The increase in IRβ levels in tissues is higher in 50-day-old *Pcmt1*–/– mice than in 20-day-old *Pcmt1*–/– mice; compare panels C and D ($n = 4$ for both *Pcmt1*+/+ and *Pcmt1*–/– mice for each liver and heart; $n = 2$ for testes). A–D, error bars represent ± SEM for all values, $*P < 0.05$, $**P < 0.005$, $***P < 0.0005$; Western blots using antibodies against actin were performed to ensure equal loading.

mice (Fig. 9B). Although the difference is not as statistically significant in newborn pups, it appears that the IRβ protein levels are high in *Pcmt1*–/– mice from a very young age, and this increase may precede the occurrence of generalized seizures observed in older animals.

To determine whether the increase in IRβ protein levels was limited to brain tissue, we conducted Western blotting experiments on extracts from liver, heart and testes from 20- and 50-day-old *Pcmt1*–/– and *Pcmt1*+/+ mice. These experiments indicated that there was an increase in IRβ protein levels in these peripheral tissues in both 20- and 50-day-old *Pcmt1*–/– mice compared with age-matched *Pcmt1*+/+ mice (Fig. 9C,D). At either age, however, the increase in IRβ protein levels was higher in the brain than in any of the peripheral tissues examined. In addition, relative IRβ protein levels in all of the tissues examined from *Pcmt1*–/– mice at 50 days of age were somewhat higher than those at 20 days of age (Fig. 9C,D), suggesting that this is both a progressive and a systemic condition.

Mild impairment in glucose tolerance without hypoinsulinaemia in *Pcmt1*–/– mice

One possible explanation for a systemic increase in insulin receptor protein levels is a decrease in blood insulin levels, as insulin is capable of regulating the expression of its own receptor (Gavin *et al.*, 1974; Kahn *et al.*, 1978). Therefore, we conducted glucose tolerance tests with glucose and insulin level measurements to determine if the *Pcmt1*–/– mice were hypoinsulinemic. These tests showed that the insulin levels in 50-day-old *Pcmt1*–/– mice were not significantly different from those of age-matched *Pcmt1*+/+ mice and were actually somewhat higher at later time points of the test (Fig. 10A). This suggests that the increase in IRβ protein levels does not result from a hypoinsulinemic condition in the *Pcmt1*–/– mice. In addition, blood glucose concentrations after fasting and 2 h after glucose ingestion were similar in *Pcmt1*–/– and *Pcmt1*+/+ mice, indicating that *Pcmt1*–/– mice were not generally hyperglycemic. However, blood glucose levels were significantly higher in *Pcmt1*–/– mice compared with *Pcmt1*+/+ mice at the earlier periods of 15 and 30 min after glucose ingestion, suggesting a mild impairment in glucose tolerance in *Pcmt1*–/– mice at 50 days of age (Fig. 10B).

Discussion

In this study we have found evidence for increased activation of the PI3K/Akt signal transduction pathway in the hippocampus and cortex of *Pcmt1*–/– mice as indicated by increased immunoreactivity for the phosphorylated forms of Akt, GSK3β

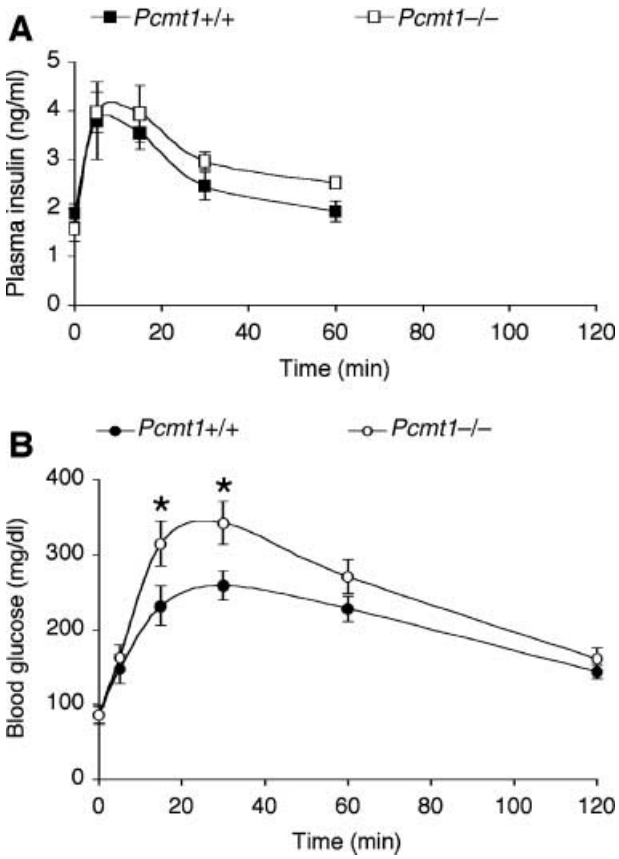

Fig. 10 Blood insulin and glucose levels during glucose tolerance tests of *Pcmt1–/–* and *Pcmt1+/+* mice. (A) Plasma insulin levels at 0, 5, 15, 30 and 60 min after glucose ingestion show similar levels of insulin at each time point for *Pcmt1+/+* and *Pcmt1–/–* mice ($n = 3$ at each time point for both *Pcmt1+/+* and *Pcmt1–/–* mice). (B) Whole blood glucose levels at 0, 5, 15, 30, 60 and 120 min after glucose ingestion show increased glucose levels in *Pcmt1–/–* mice at 15 and 30 min compared with *Pcmt1+/+* mice ($n = 9$ at each time point for both *Pcmt1+/+* and *Pcmt1–/–* mice). A and B, error bars represent ± SEM for all values, $*P < 0.05$.

and PDK-1. Additionally, there was increased immunoreactivity for the phosphorylated forms of upstream proteins IRS-1 and IGF-IR and/or IR in the hippocampus and cerebral cortex of *Pcmt1–/–* mice compared with *Pcmt1+/+* mice. Alterations in upstream or downstream components of the PI3K/Akt signal transduction pathway have previously been demonstrated in other mouse models with partial or generalized increases in brain size (Carson *et al*., 1993; Fero *et al*., 1996; Kuida *et al*., 1998; Groszer *et al*., 2001; Chenn & Walsh, 2002; Uhlmann *et al*., 2002), suggesting that the observed change in this pathway's activation in *Pcmt1–/–* mice may help to explain their progressive increase in brain size.

Increased immunohistochemical labeling of phosphorylated components of the PI3K/Akt pathway was particularly striking in the granule cells of the dentate gyrus and their mossy fibers. The dentate gyrus is one of the few regions of the adult brain in which neurons continue to be generated throughout life (Altman & Das, 1965; Gage *et al*., 1998). Changes in the PI3K/Akt pathway in this particular region could potentially increase the survival and growth of newly generated granule cells and their developing axons. In fact, in a study in which IGF-I was administered to rats, increased neurogenesis and survival was observed in the progeny of adult neural progenitor cells within the granule cell layer of the dentate gyrus (Aberg *et al*., 2000). In addition, it is possible that increased activation of this pathway could also contribute to the hyperexcitability of the mossy fiber path that has been described previously in *Pcmt1–/–* mice (Ikegaya *et al*., 2001).

Increased activation or numbers of certain receptor tyrosine kinases has been observed following epileptogenesis, as has been reported for the trkB receptor in kindled mice (He *et al*., 2002). Therefore, it is possible that the increased levels of insulin receptor and activation of the PI3K/Akt pathway could result from the seizures experienced by the *Pcmt1–/–* mice. However, we have shown that 50-day-old *Pcmt1–/–* mice have highly increased protein levels of insulin receptor in all regions of the brain and in peripheral tissues, including heart, liver and testes. In addition, we found increased insulin receptor protein levels in whole brain and peripheral tissue homogenates of *Pcmt1–/–* mice as young as 20 days of age, which is prior to the age at which generalized seizures are observed. These findings suggest that the increase in the insulin receptor protein is most likely not a consequence of the seizures observed in these mice. Furthermore, they indicate that an alteration in the insulin receptor pathway may be one of the earliest phenotypes noted in these mice.

At this point, it is unclear whether the insulin receptor is responsible for the increased phosphorylation of IRS-1 and/or the activation of the PI3K/Akt signal transduction pathway in the hippocampus and cerebral cortex of *Pcmt1–/–* mice. For example, it is possible that increased phosphorylation of IRS-1 is initiated through activation of the IGF-I receptor. However, one phenotype associated with increased IGF-I receptor activation is higher levels of myelin basic protein in the brain (Carson *et al*., 1993; Ye *et al*., 1995a,b), a phenotype which we did not detect in *Pcmt1–/–* mice as determined by Western blotting experiments (data not shown). Even if another receptor or downstream component is responsible for the increased activation of IRS-1 and the PI3K/Akt pathway, the fact that the insulin receptor levels are considerably altered in *Pcmt1–/–* mice indicates a specific variance within the insulin pathway.

To test for alterations in insulin response or glucose uptake in the *Pcmt1–/–* mice, glucose tolerance tests were performed. Although the *Pcmt1–/–* mice did not appear to have significantly altered insulin levels during these tests, the higher whole blood levels of glucose at early time points suggest a possible impairment in glucose tolerance and could be indicative of lower cellular uptake or metabolism of glucose. Therefore, in future experiments it will be important to look at downstream elements of the insulin pathway, such as glucose transporters, in the *Pcmt1–/–* mice. It is interesting to note that humans with a defective GLUT1 glucose transporter have infantile seizures (Klepper *et al*., 1999), and mice with GLUT4 selectively knocked out in heart tissue have increased insulin receptor protein levels and hypertrophy of heart cells (Abel *et al*., 1999).

One way in which PCMT1 could act as a regulator of the insulin pathway may be through its ability to limit isoaspartyl damage within cells. The lack of PCMT1 in mice causes significant accumulation of isoaspartyl-containing proteins in various tissues (Kim *et al*., 1997; Yamamoto *et al*., 1998; Lowenson *et al*., 2001), which could potentially cause alterations in the amino acid pool within cells. The cellular availability of amino acids is mainly regulated by the mammalian target of rapamycin (mTOR) through its interaction with the insulin pathway (Ozes *et al*., 2001). If amino acid availability is sufficient, mTOR induces the serine phosphorylation of IRS-1, allowing it to uncouple from the insulin receptor, thereby inhibiting insulin signaling. Therefore, if there is a high level of protein damage due to isoaspartyl accumulation, one might expect alterations in the amino acid pool that could effect mTOR's phosphorylation of IRS-1 and a subsequent regulation of the insulin pathway (Fig. 1). Therefore, in future experiments it would also be valuable to investigate the state of mTOR and the serine phosphorylation of IRS-1 in *Pcmt1–/–* mice.

Finally, in the early literature, PCMT1 was shown to have high activity in the pituitary, and all anterior pituitary hormones were shown to be effective substrates for the enzyme *in vitro* (Diliberto & Axelrod, 1974). It is well established that altered levels of growth hormone and other hormones of the anterior pituitary can alter insulin receptor levels (Landgraf *et al*., 1977; Davidson, 1987; Dominici *et al*., 2002). Therefore, it is possible that the lack of PCMT1 could influence anterior pituitary function and cause a change in the metabolic state of multiple tissues. Regardless, this study demonstrates that mice lacking PCMT1 have altered protein levels or activation of components of the insulin and/or IGF-I pathway and suggests that PCMT1 may be a critical regulator of cellular metabolism and growth.

Experimental procedures

Generation of *Pcmt1*+/+ and *Pcmt1*–/– mice

The *Pcmt1*+/+ and *Pcmt1–/–* mice were generated as previously described (Kim *et al*., 1997). By inbreeding mice that were heterozygous for the knockout mutation for many generations, a congenic mutant line has been generated that is approximately 50% 129/svJae and 50% C57BL/6. All *Pcmt1–/–* mice used in the following studies were compared with their *Pcmt1*+/+ littermates. Both male and female mice were included in the same data sets, with approximately the same number of each sex used for each genotype. Mice were weaned at 20 days of age, housed in a barrier facility with a 12-h light/dark cycle, and had unlimited access to chow food (NIH-31 Modified Mouse/Rat Diet no. 7013) and fresh water. Mice were monitored by on-site veterinarians and all protocols were pre-approved by the UCLA Animal Research Committee.

Antibodies

Polyclonal antiserum against actin was a generous gift of Dr Emil Reisler and was prepared using the peptide antigen KAGFAGDDAPRAY that includes the conserved residues 18–29 of actin proteins (Adams *et al*., 1990). These antibodies were used for Western blotting and immunohistochemistry. All other antisera used in immunohistochemical and Western blotting experiments were obtained from commercial sources. Details concerning their sources, specific antigens and dilutions are summarized in Table 1. Shaded boxes in Fig. 1 indicate all of the proteins examined by immunohistochemistry or Western blotting in this study.

For analysis of Akt in hippocampal extracts, Western blots were performed using antisera that recognized Akt and Akt phosphorylated at threonine-308. In immunohistochemical studies, an antiserum that recognized Akt phosphorylated at serine-473 was used. The downstream Akt target glycogen synthase kinase-3β was detected in immunohistochemical studies with antisera to glycogen synthase kinase-3β and glycogen synthase kinase-3β phosphorylated at serine-9. Components upstream of Akt were detected by Western blot analysis with antisera that recognized phosphoinositol-dependent kinase-1 phosphorylated at serine-241 and PTEN phosphorylated at serine-380.

Insulin receptor-related components upstream of PI3K were detected with antisera that recognized each of the following:

Table 1 Antisera used for immunohistochemistry (IHC) and Western blotting (WB)

Antisera[a]	Antigen size (kDa)	Source[b]	Catalogue no.	IHC dilution	WB dilution
pAkt (Ser473) IHC specific	60	Cell Signaling	9277	1 : 200	–
pAkt (Thr308)	60	Cell Signaling	9275	–	1 : 1000
Akt	60	Cell Signaling	9275	–	1 : 1000
GSK3	46	Cell Signaling	9332	1 : 100	–
pGSK3 (Ser9)	46	Cell Signaling	9336	1 : 100	–
pPDK1 (Ser241)	58–68	Cell Signaling	3061	–	1 : 1000
pPTEN (Ser380)	54	Cell Signaling	9551	–	1 : 2000
pIRS-1 (Tyr941)	185	Santa Cruz Biotechnology	17199	1 : 1000	–
pIGF-IR/pIR (Tyr1131/1146)	90	Cell Signaling	3021	1 : 100	–
IGF-IRβ	90	Santa Cruz Biotechnology	713	–	1 : 200
IRβ	90	Santa Cruz Biotechnology	711	–	1 : 200

[a]All produced in rabbits.
[b]Polyclonal Cell Signaling, Beverly, MA, USA; Santa Cruz Biotechnology, Santa Cruz, CA, USA.

insulin receptor substrate-1 phosphorylated at tyrosine-941, insulin-like growth factor-I receptor phosphorylated at tyrosine-1131/insulin receptor phosphorylated at tyrosine-1146 for immunohistochemistry, IGF-I receptor beta subunit and insulin receptor beta subunit for Western blot analysis.

Tissue preparation for immunohistochemistry

Two male and one female *Pcmt1–/–* mice 40–45 days old and three sex- and age-matched littermate *Pcmt1+/+* mice were used for immunohistochemical studies. The mice were deeply anaesthetized with sodium pentobarbital (90 mg kg^{-1}, i.p.) and perfused through the ascending aorta with 4% paraformaldehyde in 0.1 M sodium phosphate buffer (pH 7.3). After perfusion, the brains were maintained *in situ* at 4 °C for 1 h and then removed and postfixed in the same fixative for 1 h. After thorough rinsing in phosphate buffer, the brains were cryoprotected in a 30% sucrose solution, blocked in the coronal plane, frozen on dry ice and sectioned at 30 μm on a cryostat. Individual sections were stored in cryoprotectant solution at –20 °C until processing.

Immunohistochemical methods

Free-floating sections were processed for immunohistochemistry with standard avidin–biotin–peroxidase methods (Vectastain Elite ABC; Vector Laboratories, Burlingame, CA, USA). Sections were incubated in 10% normal goat serum in 0.1 M Tris/HCl, 1% NaCl, pH 7.4 (TBS), containing 0.3 or 1% Triton X-100 for 1 h. The sections were then incubated in the primary antibody diluted with TBS containing 2% normal goat serum overnight at room temperature. After rinsing in TBS, the sections were incubated in biotinylated goat anti-rabbit IgG (1 : 1000) at room temperature for 1 h, rinsed in TBS and incubated in ABC Elite solution (5 μL mL^{-1}) for 1 h. After rinsing in 0.075 M sodium phosphate, 1% NaCl, pH 7.3 (PBS), the sections were processed with 0.06% 3,3′-diaminobenzidene/HCl and 0.006% H_2O_2 diluted in PBS for 5–15 min. After thorough rinsing, the sections were mounted on gelatin-coated slides, dehydrated and coverslipped. In all experiments designed to compare the immunohistochemical labeling in *Pcmt1–/–* and *Pcmt1+/+* mice, sections from the two groups of animals were processed identically and in parallel for each step of the immunohistochemical procedures.

Tissue preparation for Western blotting

Brain and other tissues from 0- to 50-day-old *Pcmt1–/–* and *Pcmt1+/+* mice were extracted, weighed and immediately homogenized with 4 mL per gram of 0.1 M Tris-HCl, 1% NaCl, pH 7.4, containing 1% Triton-X 100 and protease inhibitors (one 'complete, mini, EDTA-free protease inhibitor mixture' tablet per 7 mL of buffer; Roche Diagnostics). Extracted tissues were disrupted in a glass homogenization tube with a motor-driven Teflon-coated pestle rotating at 310 r.p.m. for seven 10-s intervals. The homogenized extracts were centrifuged at 10 000 ***g*** for 30 min at 4 °C, and the resulting supernatants were stored at –20 °C until analysis.

For analysis of different brain regions for Western blotting and weight determinations, dissection of the brain was performed on ice and completed within 5 min. The brains were dissected into five regions as follows: brain stem (including pons and midbrain), cerebellum, hippocampus, thalamus/hypothalamus and cerebral cortex/basal ganglia. Homogenization and centrifugation were performed as described above.

Western blotting methods

The same tissue extracts from four *Pcmt1+/+* and four *Pcmt1–/–* mice at comparable ages were used for all Western blotting experiments. Extracts were subjected to sodium dodecyl sulphate–polyacrylamide gel electrophoresis in different slots of the same 10% polyacrylamide gel. Protein load was optimized for each antibody and ranged from approximately 10 to 50 μg based on absorbance at 280 nm. Proteins were blotted to Hybond-P membranes (Amersham Bioscience, UK) using a tank electroblotter (Owl Separation Systems, Portsmouth, NH, USA). Coomassie staining of the gel after blotting showed complete transfer of all proteins under approximately 250 kDa. Membranes were blocked with 5% dehydrated milk in TBS for 1 h at room temperature and incubated in primary antibody overnight at 4 °C. After rinsing with TBS containing 1% Tween-20 (TBS-T), membranes were incubated in horseradish peroxidase-conjugated goat anti-rabbit secondary antibody (Amersham Biosciences, UK) for 2 h at room temperature. After rinsing with TBS-T, membranes were exposed to the ECL chemiluminescent substrate (Amersham Biosciences, UK) for 1 min. The chemiluminescent signal was quantified by exposure to Kodak X-OMAT AR film followed by digital scanning using a Jade scanner (Linotype-Hell, Germany) and densitometry using NIH image software. Different exposures of the same membrane were quantified to ensure that the measured signal was in the linear range of the X-ray film. To test for equal protein loading, densitometry of Coomassie-stained gels with the same load volume as that for the Western blotting was performed. Densitometry results indicated equal protein loading for all Western blots reported here. Additionally, control Western blots using antibodies against actin were performed to ensure equivalent transfer to the membrane and equivalent reactivity of the immunological reagents.

Oral glucose-tolerance test and glucose measurements

Nine *Pcmt1+/+* mice and nine *Pcmt1–/–* mice of approximately 50 days of age were fasted overnight (15 h). A blood sample was collected from the tail vein (10 μL) immediately before glucose load (2 g glucose per kilogram of body weight) by oral administration. Blood samples were also taken at 5, 15, 30, 60 and 120 min following glucose load. Whole blood glucose levels were measured with a validated One Touch Ultra glucose measurement system (Lifescan Inc.).

Plasma insulin measurements

Whole blood (50 μL) was collected into EDTA-coated capillary tubes (VWR) from the tail vein of three *Pcmt1*+/+ mice and three *Pcmt1*–/– mice after a 15-h overnight fast and at 5, 15, 30 and 60 min after the glucose load of the glucose tolerance tests. The blood was then centrifuged and the plasma frozen at –20 °C until assayed for insulin. Insulin levels were measured with 25 μL of plasma using the Ultrasensitive Mouse Insulin ELISA (Diamyd Diagnostics AB, Sweden) enzyme immunoassay according to the manufacturer's instructions.

Statistical analysis

The results are expressed as ± SEM from *n* mice. Tests of significance were conducted for each data set using the unpaired two-tailed Student's *t*-test.

Acknowledgments

We thank Christine Huang for excellent assistance with the histology and figure preparation, Emil Reisler for providing actin antibodies, Dan Freeman for providing the pAkt (Ser473) antibody for preliminary experiments, and Jon Lowenson for editorial assistance and helpful discussions. This work was supported by National Institutes of Health Grants AG18000 (S.C.), GM26020 (S.C.) and NS046524 (C.R.H.) and by VA Medical Research Funds (C.R.H.).

References

Abel ED, Kaulbach HC, Tian R, Hopkins JC, Duffy J, Doetschman T, Minnemann T, Boers ME, Hadro E, Oberste-Berghaus C, Quist W, Lowell BB, Ingwall JS, Kahn BB (1999) Cardiac hypertrophy with preserved contractile function after selective deletion of GLUT4 from the heart. *J. Clin. Invest.* **104**, 1703–1714.

Aberg MA, Aberg ND, Hedbacker H, Oscarsson J, Eriksson PS (2000) Peripheral infusion of IGF-I selectively induces neurogenesis in the adult rat hippocampus. *J. Neurosci.* **20**, 2896–2903.

Adams S, DasGupta G, Chalovich JM, Reisler E (1990) Immunological evidence for the binding of caldesmon to the NH2-terminal segment of actin. *J. Biol. Chem.* **265**, 19652–19657.

Alessi DR, James SR, Downes CP, Holmes AB, Gaffney PR, Reese CB, Cohen P (1997) Characterization of a 3-phosphoinositide-dependent protein kinase which phosphorylates and activates protein kinase Balpha. *Curr. Biol.* **7**, 261–269.

Altman J, Das GD (1965) Autoradiographic and histological evidence of postnatal hippocampal neurogenesis in rats. *J. Comp. Neurol.* **124**, 319–335.

Baserga R (1999) The IGF-I receptor in cancer research. *Exp. Cell. Res.* **253**, 1–6.

Baskin DG, Figlewicz DP, Woods SC, Porte D Jr, Dorsa DM (1987) Insulin in the brain. *Annu. Rev. Physiol.* **49**, 335–347.

Brennan TV, Anderson JW, Jia Z, Waygood EB, Clarke S (1994) Repair of spontaneously deamidated HPr phosphocarrier protein catalyzed by the 1-isoaspartate-(D-aspartate) O-methyltransferase. *J. Biol. Chem.* **269**, 24586–24595.

Carson MJ, Behringer RR, Brinster RL, McMorris FA (1993) Insulin-like growth factor I increases brain growth and central nervous system myelination in transgenic mice. *Neuron* **10**, 729–740.

Casamayor A, Morrice NA, Alessi DR (1999) Phosphorylation of Ser-241 is essential for the activity of 3-phosphoinositide-dependent protein kinase-1: identification of five sites of phosphorylation in vivo. *Biochem. J.* **342**, 287–292.

Chavous DA, Jackson FR, O'Connor CM (2001) Extension of the *Drosophila* lifespan by overexpression of a protein repair methyltransferase. *Proc. Natl. Acad. Sci. USA* **98**, 14814–14818.

Cheng X, Ma Y, Moore M, Hemmings BA, Taylor SS (1998) Phosphorylation and activation of cAMP-dependent protein kinase by phosphoinositide-dependent protein kinase. *Proc. Natl Acad. Sci. USA* **95**, 9849–9854.

Chenn A, Walsh CA (2002) Regulation of cerebral cortical size by control of cell cycle exit in neural precursors. *Science* **297**, 365–369.

Cross DA, Alessi DR, Cohen P, Andjelkovich M, Hemmings BA (1995) Inhibition of glycogen synthase kinase-3 by insulin mediated by protein kinase B. *Nature* **378**, 785–789.

Datta SR, Brunet A, Greenberg ME (1999) Cellular survival: a play in three Akts. *Genes Dev.* **13**, 2905–2927.

Davidson MB (1987) Effect of growth hormone on carbohydrate and lipid metabolism. *Endocr. Rev.* **8**, 115–131.

Diliberto EJ Jr, Axelrod J (1974) Characterization and substrate specificity of a protein carboxymethylase in the pituitary gland. *Proc. Natl Acad. Sci. USA* **71**, 1701–1704.

Dominici FP, Hauck S, Argentino DP, Bartke A, Turyn D (2002) Increased insulin sensitivity and upregulation of insulin receptor, insulin receptor substrate (IRS)-1 and IRS-2 in liver of Ames dwarf mice. *J. Endocrinol.* **173**, 81–94.

Doyle HA, Gee RJ, Mamula MJ (2003) A failure to repair self-proteins leads to T cell hyperproliferation and autoantibody production. *J. Immunol.* **171**, 2840–2847.

Fero ML, Rivkin M, Tasch M, Porter P, Carow CE, Firpo E, Polyak K, Tsai LH, Broudy V, Perlmutter RM, Kaushansky K, Roberts JM (1996) A syndrome of multiorgan hyperplasia with features of gigantism, tumorigenesis, and female sterility in p27 (Kip1)-deficient mice. *Cell* **85**, 733–744.

Gage FH, Kempermann G, Palmer TD, Peterson DA, Ray J (1998) Multipotent progenitor cells in the adult dentate gyrus. *J. Neurobiol.* **36**, 249–266.

Gavin JR, 3rd, Roth J, Neville DM Jr, de Meyts P, Buell DN (1974) Insulin-dependent regulation of insulin receptor concentrations: a direct demonstration in cell culture. *Proc. Natl Acad. Sci. USA* **71**, 84–88.

Groszer M, Erickson R, Scripture-Adams DD, Lesche R, Trumpp A, Zack JA, Kornblum HI, Liu X, Wu H (2001) Negative regulation of neural stem/progenitor cell proliferation by the Pten tumor suppressor gene in vivo. *Science* **294**, 2186–2189.

Havrankova J, Roth J, Brownstein M (1978) Insulin receptors are widely distributed in the central nervous system of the rat. *Nature* **272**, 827–829.

He XP, Minichiello L, Klein R, McNamara JO (2002) Immunohistochemical evidence of seizure-induced activation of trkB receptors in the mossy fiber pathway of adult mouse hippocampus. *J. Neurosci.* **22**, 7502–7508.

Hernandez-Sanchez C, Blakesley V, Kalebic T, Helman L, LeRoith D (1995) The role of the tyrosine kinase domain of the insulin-like growth factor-I receptor in intracellular signaling, cellular proliferation, and tumorigenesis. *J. Biol. Chem.* **270**, 29176–29181.

Huebscher KJ, Lee J, Rovelli G, Ludin B, Matus A, Stauffer D, Furst P (1999) Protein isoaspartyl methyltransferase protects from Bax-induced apoptosis. *Gene* **240**, 333–341.

Ikegaya Y, Yamada M, Fukuda T, Kuroyanagi H, Shirasawa T, Nishiyama N (2001) Aberrant synaptic transmission in the hippocampal CA3 region

and cognitive deterioration in protein-repair enzyme-deficient mice. *Hippocampus* **11**, 287–298.

Ingrosso D, D'Angelo S, di Carlo E, Perna AF, Zappia V, Galletti P (2000) Increased methyl esterification of altered aspartyl residues in erythrocyte membrane proteins in response to oxidative stress. *Eur. J. Biochem.* **267**, 4397–4405.

Johnson BA, Murray ED Jr, Clarke S, Glass DB, Aswad DW (1987) Protein carboxyl methyltransferase facilitates conversion of atypical 1-isoaspartyl peptides to normal 1-aspartyl peptides. *J. Biol. Chem.* **262**, 5622–5629.

Kahn CR, Goldfine ID, Neville DM Jr, De Meyts P (1978) Alterations in insulin binding induced by changes in vivo in the levels of glucocorticoids and growth hormone. *Endocrinology* **103**, 1054–1066.

Kim E, Lowenson JD, Clarke S, Young SG (1999) Phenotypic analysis of seizure-prone mice lacking 1-isoaspartate (D-aspartate) O-methyltransferase. *J. Biol. Chem.* **274**, 20671–20678.

Kim E, Lowenson JD, MacLaren DC, Clarke S, Young SG (1997) Deficiency of a protein-repair enzyme results in the accumulation of altered proteins, retardation of growth, and fatal seizures in mice. *Proc. Natl Acad. Sci. USA* **94**, 6132–6137.

Klepper J, Wang D, Fischbarg J, Vera JC, Jarjour IT, O'Driscoll KR, De Vivo DC (1999) Defective glucose transport across brain tissue barriers: a newly recognized neurological syndrome. *Neurochem. Res.* **24**, 587–594.

Kozma SC, Thomas G (2002) Regulation of cell size in growth, development and human disease: PI3K, PKB and S6K. *Bioessays* **24**, 65–71.

Kuida K, Haydar TF, Kuan CY, Gu Y, Taya C, Karasuyama H, Su MS, Rakic P, Flavell RA (1998) Reduced apoptosis and cytochrome c-mediated caspase activation in mice lacking caspase 9. *Cell* **94**, 325–337.

Landgraf R, Landraf-Leurs MM, Weissmann A, Horl R, von Werder K, Scriba PC (1977) Prolactin: a diabetogenic hormone. *Diabetologia* **13**, 99–104.

Lanthier J, Desrosiers RR (2004) Protein 1-isoaspartyl methyltransferase repairs abnormal aspartyl residues accumulated in vivo in type-I collagen and restores cell migration. *Exp. Cell Res.* **293**, 96–105.

Lopaczynski W, Terry C, Nissley P (2000) Autophosphorylation of the insulin-like growth factor I receptor cytoplasmic domain. *Biochem. Biophys. Res. Commun.* **279**, 955–960.

Lowenson JD, Kim E, Young SG, Clarke S (2001) Limited accumulation of damaged proteins in 1-isoaspartyl (D-aspartyl) O-methyltransferase-deficient mice. *J. Biol. Chem.* **276**, 20695–20702.

Maehama T, Dixon JE (1998) The tumor suppressor, PTEN/MMAC1, dephosphorylates the lipid second messenger, phosphatidylinositol 3,4,5-trisphosphate. *J. Biol. Chem.* **273**, 13375–13378.

McFadden PN, Clarke S (1987) Conversion of isoaspartyl peptides to normal peptides: implications for the cellular repair of damaged proteins. *Proc. Natl Acad. Sci. USA* **84**, 2595–2599.

Miller SJ, Lou DY, Seldin DC, Lane WS, Neel BG (2002) Direct identification of PTEN phosphorylation sites. *FEBS Lett.* **528**, 145–153.

Ozes ON, Akca H, Mayo LD, Gustin JA, Maehama T, Dixon JE, Donner DB (2001) A phosphatidylinositol 3-kinase/Akt/mTOR pathway mediates and PTEN antagonizes tumor necrosis factor inhibition of insulin signaling through insulin receptor substrate-1. *Proc. Natl Acad. Sci. USA* **98**, 4640–4645.

Scheid MP, Woodgett JR (2003) Unravelling the activation mechanisms of protein kinase B/Akt. *FEBS Lett.* **546**, 108–112.

Srivastava AK, Pandey SK (1998) Potential mechanism(s) involved in the regulation of glycogen synthesis by insulin. *Mol. Cell Biochem.* **182**, 135–141.

Steinberg RA, Cauthron RD, Symcox MM, Shuntoh H (1993) Autoactivation of catalytic (C alpha) subunit of cyclic AMP-dependent protein kinase by phosphorylation of threonine 197. *Mol. Cell Biol.* **13**, 2332–2341.

Stephens L, Anderson K, Stokoe D, Erdjument-Bromage H, Painter GF, Holmes AB, Gaffney PR, Reese CB, McCormick F, Tempst P, Coadwell J, Hawkins PT (1998) Protein kinase B kinases that mediate phosphatidylinositol 3,4,5-trisphosphate-dependent activation of protein kinase B. *Science* **279**, 710–714.

Torres J, Pulido R (2001) The tumor suppressor PTEN is phosphorylated by the protein kinase CK2 at its C terminus. Implications for PTEN stability to proteasome-mediated degradation. *J. Biol. Chem.* **276**, 993–998.

Uhlmann EJ, Wong M, Baldwin RL, Bajenaru ML, Onda H, Kwiatkowski DJ, Yamada K, Gutmann DH (2002) Astrocyte-specific TSC1 conditional knockout mice exhibit abnormal neuronal organization and seizures. *Ann. Neurol.* **52**, 285–296.

Unger J, McNeill TH, Moxley RT, 3rd, White M, Moss A, Livingston JN (1989) Distribution of insulin receptor-like immunoreactivity in the rat forebrain. *Neuroscience* **31**, 143–157.

Unger JW, Moss AM, Livingston JN (1991) Immunohistochemical localization of insulin receptors and phosphotyrosine in the brainstem of the adult rat. *Neuroscience* **42**, 853–861.

Vazquez F, Grossman SR, Takahashi Y, Rokas MV, Nakamura N, Sellers WR (2001) Phosphorylation of the PTEN tail acts as an inhibitory switch by preventing its recruitment into a protein complex. *J. Biol. Chem.* **276**, 48627–48630.

White MF (1998) The IRS-signaling system: a network of docking proteins that mediate insulin action. *Mol. Cell. Biochem.* **182**, 3–11.

White MF, Shoelson SE, Keutmann H, Kahn CR (1988) A cascade of tyrosine autophosphorylation in the beta-subunit activates the phosphotransferase of the insulin receptor. *J. Biol. Chem.* **263**, 2969–2980.

White MF, Takayama S, Kahn CR (1985) Differences in the sites of phosphorylation of the insulin receptor in vivo and in vitro. *J. Biol. Chem.* **260**, 9470–9478.

White MF, Yenush L (1998) The IRS-signaling system: a network of docking proteins that mediate insulin and cytokine action. *Curr. Top. Microbiol. Immunol.* **228**, 179–208.

Xu B, Bird VG, Miller WT (1995) Substrate specificities of the insulin and insulin-like growth factor 1 receptor tyrosine kinase catalytic domains. *J. Biol. Chem.* **270**, 29825–29830.

Yamamoto A, Takagi H, Kitamura D, Tatsuoka H, Nakano H, Kawano H, Kuroyanagi H, Yahagi Y, Kobayashi S, Koizumi K, Sakai T, Saito K, Chiba T, Kawamura K, Suzuki K, Watanabe T, Mori H, Shirasawa T (1998) Deficiency in protein 1-isoaspartyl methyltransferase results in a fatal progressive epilepsy. *J. Neurosci.* **18**, 2063–2074.

Ye P, Carson J, D'Ercole AJ (1995a) In vivo actions of insulin-like growth factor-I (IGF-I) on brain myelination: studies of IGF-I and IGF binding protein-1 (IGFBP-1) transgenic mice. *J. Neurosci.* **15**, 7344–7356.

Ye P, Carson J, D'Ercole AJ (1995b) Insulin-like growth factor-I influences the initiation of myelination: studies of the anterior commissure of transgenic mice. *Neurosci. Lett.* **201**, 235–238.